Journal of Volcanology and Geothermal Research 401 (2020) 106947

Contents lists available at ScienceDirect

Journal of Volcanology and Geothermal Research

journal homepage: www.elsevier.com/locate/jvolgeores

The 1951 eruption of Mount Lamington, Papua New Guinea: Devastating directed blast triggered by small-scale edifice failure

Belousov Alexander [a,*], Belousova Marina [a], Hoblitt Richard [b], Patia Herman [c,1]

[a] Institute of Volcanology and Seismology, Piip boulevard 9, Petropavlovsk-Kamchatsky 683006, Russia
[b] Cascades Volcano Observatory, Vancouver, WA 98683, United States of America
[c] Rabaul Volcano Observatory, Rabaul 2530, Papua New Guinea

ARTICLE INFO

Article history:
Received 23 February 2020
Received in revised form 15 May 2020
Accepted 28 May 2020
Available online 02 June 2020

ABSTRACT

The catastrophic explosion of Mount Lamington volcano, Papua New Guinea on January 21, 1951 produced a devastating pyroclastic density current (PDC) that knocked down dense tropical rainforest over an area of 230 km^2 and killed approximately 3000 people. We present results of a field reinvestigation of the 1951 PDC deposit combined with an analysis of the available photographs and eyewitness accounts of the eruption first published in the fundamental work of G. A. M. Taylor (1958).

We have concluded that the six-days-long pre-climactic activity before the 1951 eruption (which included felt local seismicity, frequent ash-laden explosions of vulcanian type, bulging of the volcano slope accompanied with landslides) was associated with shallow-level intrusion of a highly viscous magma body (cryptodome/dome) of andesitic composition with a volume of approximately 0.01 km^3. This intrusion destabilized Mount Lamington's prehistoric intra-crater lava dome.

On January 21 the destabilized dome gravitationally collapsed and produced a relatively small-volume debris avalanche, the deposit of which was not recognized during Taylor's original investigation. The debris avalanche had a volume of approximately 0.02–0.04 km^3, travelled a distance (L) of 8.5 km and had the ratio of vertical drop (H) to runout (L) of 0.14. The edifice collapse decompressed the intruding cryptodome and triggered its explosive fragmentation.

Photographs of the climactic explosion show that the eruptive cloud initially rose vertically but subsequently collapsed upon the terrain around the vent, and formed a PDC which flowed radially outward. The enhanced northward propagation of the PDC to a maximum distance of 13 km reveals that the northern breach in the ancient crater's high walls influenced the distribution of the deposit. In the studied NE-N-NW sector of the devastated area, in the zone proximal to the volcano, the PDC emplaced a normally graded layer of coarse ash and lapilli mixed in the base with picked-up soil and plant fragments. The layer gradually becomes thinner and finer-grained with distance from the volcano. The PDC deposit has a volume of approximately 0.025 km^3 and consists of approximately 80% juvenile rock fragments derived from the explosively fragmented cryptodome. The remaining 20% consists of accidental clasts derived from the old volcanic edifice. The juvenile material is crystal-rich andesite with a unimodal vesicularity distribution (4 to 36%). The reconstructed eruption sequence, the PDC tree blowdown pattern and characteristics of the PDC deposit are similar to those of catastrophic laterally-directed blasts of volcanoes Bezymianny in 1956, Mount St.Helens in 1980, and Soufriere Hills, Montserrat in 1997. In contrast to the cases of these "classic" lateral blasts, the blast cloud of Lamington was initially vertically-directed before collapsing to produce a PDC. We speculate that the climactic explosion of Mount Lamington was initially vertical because the rupture surface of the triggering sector collapse intersected the apex of the intruding cryptodome (it exposed a subhorizontal surface of the cryptodome apex), while at Bezymianny, Mount St.Helens, and Soufriere Hills the rupture intersected the main body of the cryptodome/dome, and exposed their steeply inclined surfaces.

1. Introduction

The "directed blast" type of volcanic explosions was first described by G. Gorshkov (1963) who studied the 1956 eruption of Bezymianny volcano in Kamchatka, Russia (Gorshkov, 1959; Belousov, 1996). This

* Corresponding author.
E-mail address: belousov@mail.ru (B. Alexander).
[1]Passed away.

https://doi.org/10.1016/j.jvolgeores.2020.106947
0377-0273/

blast, which involved approximately 0.15 km^3 of magma, toppled and singed vegetation over an elliptically-shaped area of 500 km^2, with the volcano at one of the ellipse foci. A remarkably similar explosive event at Mount St. Helens In 1980 was described as "lateral blast" (Hoblitt et al., 1981). Comparison of these two eruptions with a much smaller blast at Soufriere Hills volcano on Montserrat in the Lesser Antilles in 1997 allowed Belousov et al., 2007 to summarize the main features of this peculiar type of volcanic eruption. Directed/lateral blasts occur under certain conditions during shallow intrusions (cryptodomes) and/or extrusions (domes) of viscous magma. A characteristic feature of a directed blast is the inclined ejection of a gas-pyroclastic mixture that initially is denser than air and thus not buoyant. Consequently, the ejected mixture gravitationally collapses and generates a highly inflated, mobile, and destructive pyroclastic density current (PDC). The inclined character of the initial ejection produces a radially asymmetric but bilaterally symmetric PDC or blast PDC (after Belousov et al., 2007). Lateral blasts at Bezymianny, Mount St. Helens and Soufriere Hills, Montserrat were all triggered by voluminous landslides (sector collapses) from the volcanoes' flanks (Belousov et al., 2007). These landslides unloaded the intruding /extruding magma body that led to its explosive fragmentation with inclined ("lateral" or "directed") ejection of the resulted gas-pyroclastic mixture oriented in the direction of the triggering landslide. These three well-documented eruptions were described in multiple research papers and thus can be called "classic" blasts. Two other notable eruptions of the 20th century that can be tentatively (because of the lack of some critical observational data about their eruption courses and deposits) classified as directed blasts are the May 8, 1902 eruption of Mount Pelée on Martinique (Lacroix, 1904) and the January 21, 1951 eruption of Mount Lamington in Papua New Guinea (Taylor, 1958).

The catastrophic explosion of Mount Lamington produced a pyroclastic density current (PDC) that knocked down dense tropical forest over an area of 230 km^2 and killed approximately 3000 people. The PDC impact—its tree blowdown pattern, estimated temperature (200 °C), and propagation velocity (27–94 m/s) (Taylor, 1958)—are similar to those of the classic blast PDCs (Belousov et al., 2007).

We present results of our field reinvestigation of the 1951 deposits combined with the analysis of the available photographs and eyewitness accounts of the eruption first published in the fundamental work of G.A.M. Taylor (1958). At the time of Taylor's study, the relationships between sector collapses, debris avalanche deposits, and lateral blasts were completely unknown. Our main goals were to study the deposits, to reconstruct the eruptive sequence of the 1951 eruption, and to access the similarity/dissimilarity to the classic lateral blasts. This comparison allows us to better understand the mechanisms of blast-generating eruptions. We also present new data constraining ages and origin of deposits that pre-date the 1951 eruption in order to place this eruption in context of the volcano's eruption history.

2. Methodology

2.1. Sampling

Our mapping and sampling of the 1951 erupted products was conducted in two field campaigns: in 1982 by R. Hoblitt (Hoblitt, 1982) and in 2010 by A.Belousov, M.Belousova, and H. Patia correspondingly in 11 and 60 locations shown on Fig. 1b. For grain size, component analyses, and density/vesicularity measurements, 113 samples (1–3 kg each, depending on the grain size of the sampled deposit) were collected (23 in 1982 and 90 in 2010).

Sampling of volcaniclastic deposits that pre-date the 1951 eruption (15 samples including 3 samples for C^{14} dating (Fig. 1a)) was conducted in 2010 in 10 locations.

2.2. Granulometry

Grain size analyses of samples of the volcaniclastic deposits were first performed by standard dry sieving techniques (Walker, 1971). Subsequently, the >4 phi unit size fraction (water suspension) was investigated using a "Fritsch Analysette 22 Compact" Laser Particle Sizer.

2.3. Component and chemical analyses

Componentry analyses were performed on the 5–30 mm size fractions (on average 30 clasts in a sample) by visually identifying and counting the various lithologic types under a binocular microscope. Surface morphology of pyroclasts was studied with scanning electron microscope JSM 6360 at Nanyang Technological University in Singapore.

XRF analyses of major and trace elements concentrations in two samples of juvenile andesite were made by Axios Advanced XRF spectrometer with 4 kW Rh tube in Earth Observatory of Singapore.

Density and vesicularity indexes of juvenile rock fragments were determined for 0.5–1 cm clasts (on average 30 clasts in a sample sprayed with waterproof spray containing silicon oil) by the method of Houghton and Wilson (1989) and Hoblitt and Harmon (1993) using the difference between the sample weights in water and air. For the calculation of the vesicularity indexes, the density of non-vesicular silicic andesite was taken as 2.7 g/m^3 (Mueller et al., 2011).

2.4. Radiocarbon dating

Three samples of charcoal and wood buried in prehistoric volcaniclastic deposits of Lamington were collected for determination of their emplacement C^{14} ages at points #1, 2 and 3 in Fig. 1a. Radiocarbon dating (Table 1) was performed by BETA Analytic radiocarbon dating laboratory using the AMS (Accelerator Mass Spectrometer) method and calibration database INTCAL09.

3. Geological framework of Mount Lamington

3.1. Regional tectonics and geology

Mount Lamington is located in the eastern part of the island of New Guinea on the Papuan Peninsula (Fig. 1a). This region has one of the most complex tectonic regimes on Earth (Fig. 2). Here the Australian Plate moving towards north-northeast obliquely collides with the Pacific Plate that moves towards west-southwest at 110 mm/year with a convergent component of 70 mm/year across the New Guinea region (Tregoning and Gorbatov, 2004). The collision led to fragmentation of the plate edges into several microplates. The microplates subsequently interacted with each other and formed relatively small, short-lived subduction zones with corresponding volcanic arcs (Baldwin et al., 2012 and references therein). The present-day active subduction occurs along the New Britain Trench where the Solomon Sea microplate plunges northward under South Bismarck microplate, generating active volcanism of the West Bismarck and New Britain arcs (jointly referred as the Bismarck arc). Four hundred kilometers south of the Bismarck arc and parallel to it, in the eastern part of the Island of New Guinea, lies another volcanic arc—the Papuan arc—that includes three volcanoes with recorded eruptions: Mount Victory (erupted in 1880s), Waiowa (Goropu) maars (erupted in 1943–44) and Mount Lamington (erupted in 1951) (Baker, 1946; Taylor, 1958; Smith, 1982). This arc is comprised of volcanic rocks ranging in age from Late Cenozoic to Recent (Smith and Compston, 1982) with compositions ranging from basalts to rhyolites; basaltic andesites and andesites are most abundant. Calc-alkaline affinity and abundant hydrous phenocrysts in the rocks suggest that the magmas of the arc maybe the products of melting of subduction-modified mantle (Johnson et al., 1978; Smith and Johnson, 1981; Arculus et al., 1983). Beneath the Papuan arc, however, there is no well-defined Benioff-Wadati zone of seismicity, and the cause of its

modern volcanism is debated. It has been attributed to slow or "silent" southward subduction of the Solomon Sea microplate at the Trobriand Trough (e.g., Hamilton, 1979; Smith, 1982; Cooper and Taylor, 1987) or to decompression melting caused by westward propagation of the Woodlark Spreading– Rifting System (Johnson et al., 1978; Woodhead et al., 2010).

The complex tectonics generated the complex geological structure of Papua: a collage of multiple obducted and subducted fragments of the interacting microplates (Baldwin et al., 2012). Lamington volcano is built on a northeast-dipping ophiolite sheet of the Papuan Ultramafic Belt overlain by Plio-Quaternary sediments (Baldwin et al., 2012).

3.2. Volcanic edifice and eruption history of Mount Lamington before the 1951 eruption

The volcanic edifice has a complex morphology (Fig. 3) composed of several overlapping steep-sided lava domes, thick lava flows, and their clastic aprons. Lavas of Mount Lamington are porphyritic trachybasalt and high-Si, medium-to-high-K andesite (Arculus et al., 1983).

The pre-1951 eruptive history of the volcano has not been studied in detail. Examination of volcaniclastic deposits exposed in ravines in the volcano's northern flank allowed Taylor (1958) to conclude that dome-forming eruptions accompanied by generation of various types

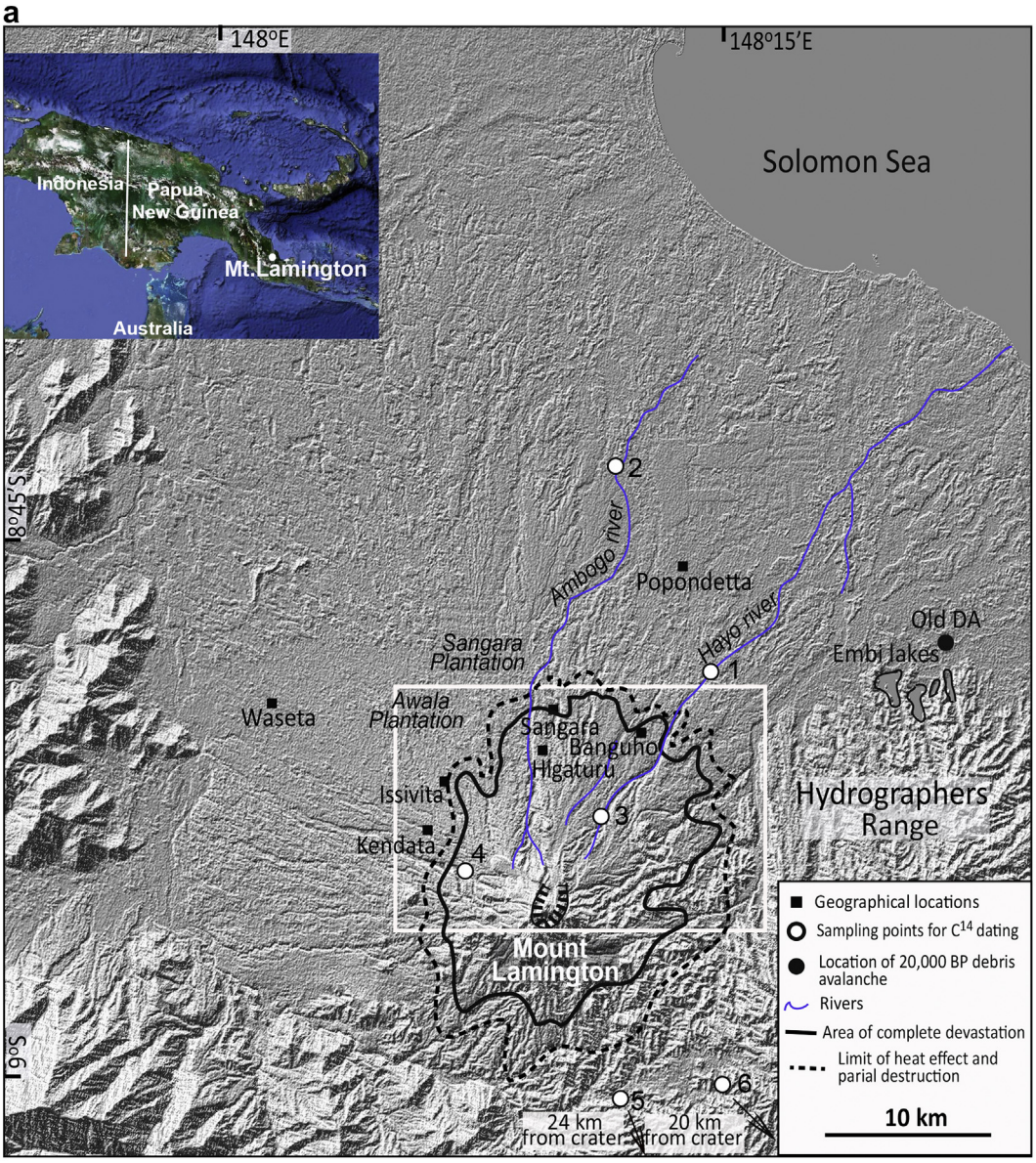

Fig. 1. (a). Sketch map of the vicinity of Mount Lamington (based on Fig. 57 from Johnson, 2013) with indicated area of devastation by the 1951 blast PDC (inner solid contour - boundary of complete devastation; outer dashed contour - boundary of partial devastation). Geographical locations mentioned in the description of the 1951 eruption and compiled in Table 2 are shown. White dots - sampling points for C^{14} dating (compiled in Table 1), black dot - location of hummocky relief of prehistoric (20,000BP) debris avalanche (DA) deposit of Mount Lamington (Fig. 3a). The insert shows location of Mount Lamington on Google image. (b) Locations of sampling points of the 1951 deposits placed over mosaic of airphotos of the 1951 devastated area (air survey on February 22, 1951). Light grey area is area devastated by blast PDC, dark grey area is undamaged forest. Triangles - the 1951 debris avalanche deposit, dots - the 1951 PDC deposit: yellow – the 1982 field campaign, blue - the 2010 field campaign. Dashed line shows approximate location of the 1951 debris avalanche front. Points described in the text are indicated.

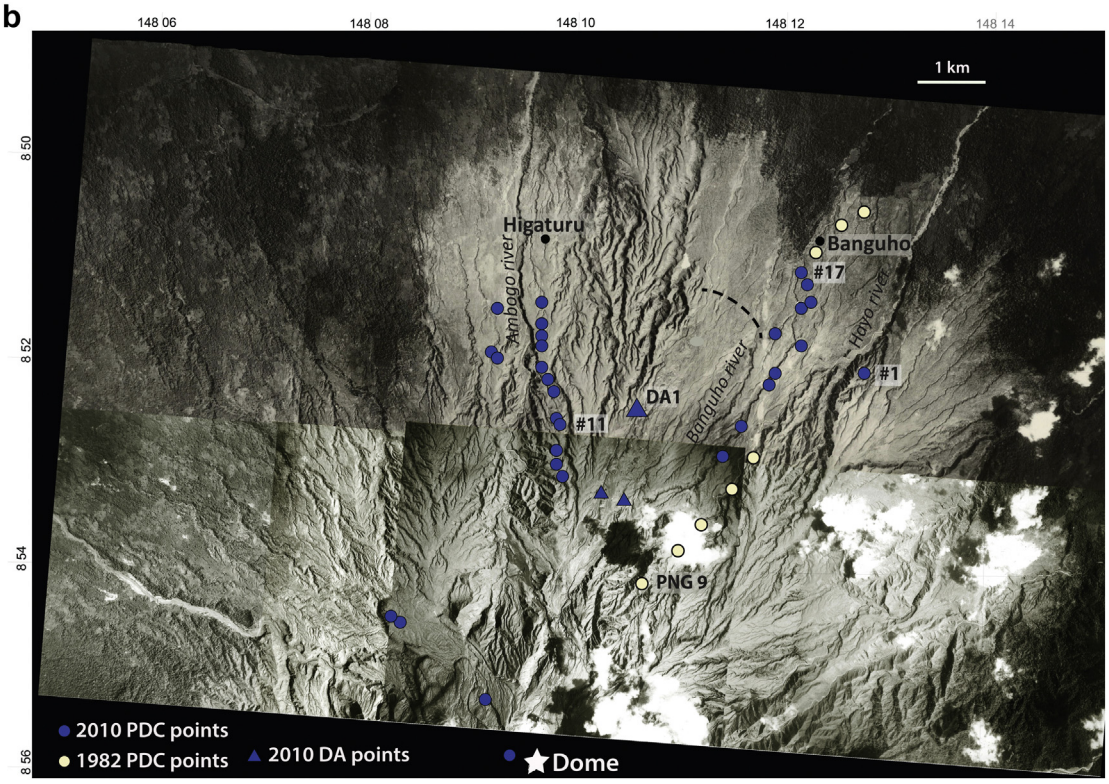

Fig. 1 (*continued*).

of PDCs ("nuées") represent the most common type of eruptive activity of Mount Lamington. The age of the volcano was estimated to be approximately 100,000 years basing on accumulation rate of ash fallout deposits (Ruxton, 1966). Before the 1951 eruption, which was Lamington's first historical activity, its central dome was nested within a 1.3 km-wide crater breached to the north (Fig. 3a). The amphitheater morphology of the crater indicates that it was probably formed by a voluminous prehistoric gravitational sector collapse (Johnson, 1987).

Table 1
Summary of radiocarbon ages (new and previously published) for Mount Lamington. Ages obtained in this study are indicated by bold italic. Sampling locations are shown in Fig. 1a.

Point #	Location	Geographical coordinates	Distance from crater, km	Dated material	Deposit/dated event	Method	Measured Age, BP	Conventional Age, BP	2 Sigma calibration	References
1	Hayo river	8°49′0.7″ 148°14′30.1″	15,5	Charcoal from PF	Large pumice PF following DA emplacement associated with formation of the pre-1951 horseshoe-shaped crater; formation of Embi lakes.	AMS	***19,830 ± 120***	***19,820 ± 120***	result is outside calibration range	Our samples, dated in Beta Analytic lab, USA
2	Ambogo river	8°45′17″ 148°12′33.2"	21,8	Wood from deposit (>2 m thick) of paleolake dammed by ancient DA		Radiometric	***18,040 ± 110***	***17,990 ± 110***	***21,295 ± 315***	
3	Bonguho river	8°52′49.5″ 148°11′27.1"	6,5	Charcoal from PF	Block and ash PF, last eruption before 1951	AMS	***2520 ± 40***	***2480 ± 40***	***2545 ± 185***	
4	Embara river		5	Carbonized wood from PF	PF associated with formation of the pre-1951 lava dome	Radiometric	13,000 ± 500			Fergusson and Rafter (1953)
5	SE from crater		20	Charcoal from ash layer	CO-PDC ash fallouts associated with formation of the pre-1951 lava dome	Radiometric	7930 ± 370			Ruxton, 1966
6	SSE from crater		24	Charcoal from ash layers depth 65 cm depth 1.5 m depth 2.2 m		Radiometric Radiometric Radiometric	6800 ± 250 15,000 ± 500 20,100 ± 500			

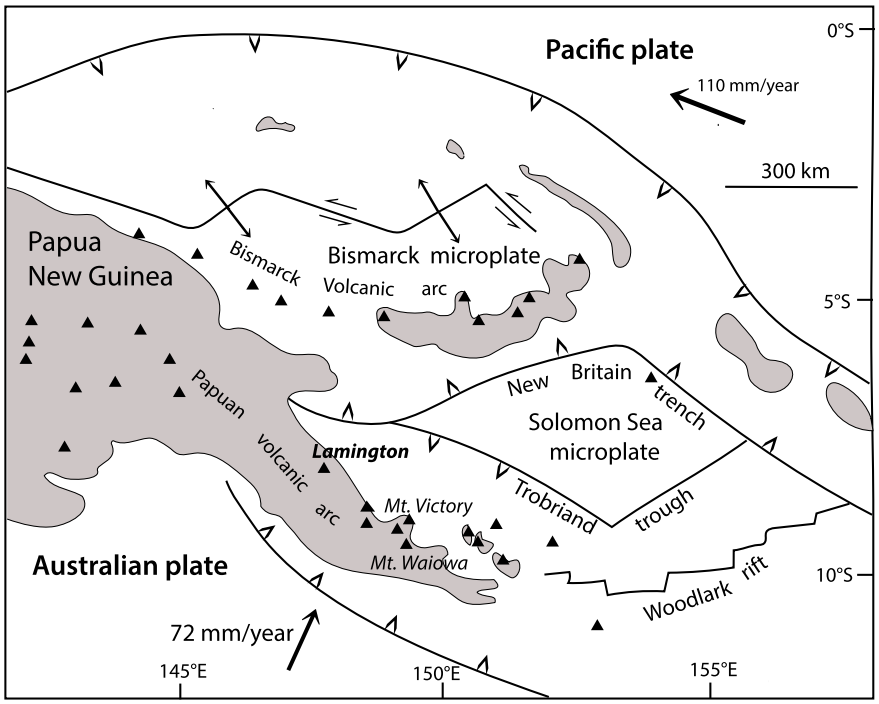

Fig. 2. Sketch of tectonic setting of southeastern Papua New Guinea, with modifications after Smith (2014).

While investigating the northern foot of the volcano we found the hummocky deposit of an ancient debris avalanche (Fig. 4), in the area immediately north of Embi Lakes at the distance 25 km from the volcano (Fig. 1a). The south-eastern lateral margin of the deposit dammed four river valleys originating at the northern slopes of the Hydrographers Range; this led to formation of the Embi Lakes. That happened about 20,000 BP, because closer to the volcano in the bank of Hayo River at point #1 (Fig. 1a), charcoal from within the stratigraphically younger deposit of a 1 m thick pumiceous pyroclastic flow yielded a conventional C^{14} age of 19,820 ±120 BP (Table 1). Similarly, a conventional C^{14} age of 17,990±110 BP was obtained at point #2 (Fig. 1a, Table 1) for a wood fragment buried in finely laminated sediment of a paleolake >2 m thick. Formation of the paleolake was probably associated with the avalanche deposition, similar to the formation of the Embi Lakes.

We estimate the volume of the debris avalanche as follows. The average H/L ratio for debris avalanches is 0.1 (Siebert, 1984). Given the observed runout distance (L) of 25 km, the difference (H) between the pre-collapse elevation of the edifice and the elevation of the avalanche front, is 0.1 × 25 km = 2.5 km. The elevation of the avalanche front near Embi Lakes lies at 60 masl., so the pre-collapse elevation of the Lamington edifice was about 2500 m + 60 m = 2560 masl. The existing rim of the collapse crater is 1500 masl, so the collapse reduced the height of the edifice by 1060 m. Assuming the pre-collapse edifice was conical, the collapse removed a cone with a base of 1300 m (that is the diameter of the ancient collapse crater) and a height of 1060 m. This cone has volume of 0.47 km^3. This is a minimum volume of the 20,000 BP debris avalanche.

Subsequently, a long period of intracrater dome growth began. As a result, the crater was partially filled by a lava dome (Fig. 3a). This dome was completely destroyed in the course of the 1951 eruption when the new horseshoe-shaped crater was formed. The location, shape and dimensions of the 1951 crater almost exactly coincided with that of the 20,000 BP crater (Figs. 3a and b).

Ruxton (1966) described a thick sequence of well-sorted, fine to medium ash layers at distances of 12–28 km ESE of Mount Lamington. Lithological characteristics of the ash and the presence of charcoal fragments in some of these layers suggest that many of them are probably co-PDC ash cloud deposits. Considering the C^{14} ages of the charcoal fragments from these co-PDC ash fallout layers obtained by Ruxton (1966) and the C^{14} age of a prehistoric pyroclastic flow obtained by Fergusson and Rafter (1953) as well as C^{14} ages of two prehistoric pyroclastic flows obtained in this study (Table 1), one can conclude that major eruptions accompanied by emplacement of PDCs, occurred about 20,000, 15,000, 13,000, 7900, 6800 and 2500 BP. These eruptions were probably associated with formation of the pre-1951 central dome of Mount Lamington, which started to grow inside the 20,000 BP collapse crater. The 2500 BP eruption probably was the last activity of the dome and the last eruption of Mount Lamington before the 1951 eruption.

4. The 1951 eruption

4.1. Pre-climactic activity

No instrumental monitoring of the volcano existed before the eruption. The available observational data on the pre-climactic activity (pp. 12–14 from Taylor (1983), 2nd edition of Taylor (1958)) and our interpretations of the volcanic phenomena are summarized in Table 2.

The first signs of the unrest were occasional slight earth tremors that residents of the settlements nearest to the volcano started to feel since the beginning of January 1951. With time these tremors became stronger and more frequent.

On January 15 multiple landslides were noticed on the summit peaks of Mount Lamington. Taylor (1958) interpreted them as the direct result of the seismic activity, however they could be caused also by ground deformations and/or indicate changes of groundwater table and/or increase of pore pressure inside the volcanic edifice that were associated with shallow intrusion of magma. The same day a column of white steam appeared at the base of the prehistoric intracrater dome.

On January 16 the steaming increased and the earthquakes became stronger and more frequent (30 shocks in 12 h when the “whole earth rocking”).

a


MT. LAMINGTON
small dome in pre-eruption crater
avalanche valley
old lava flow

b

c

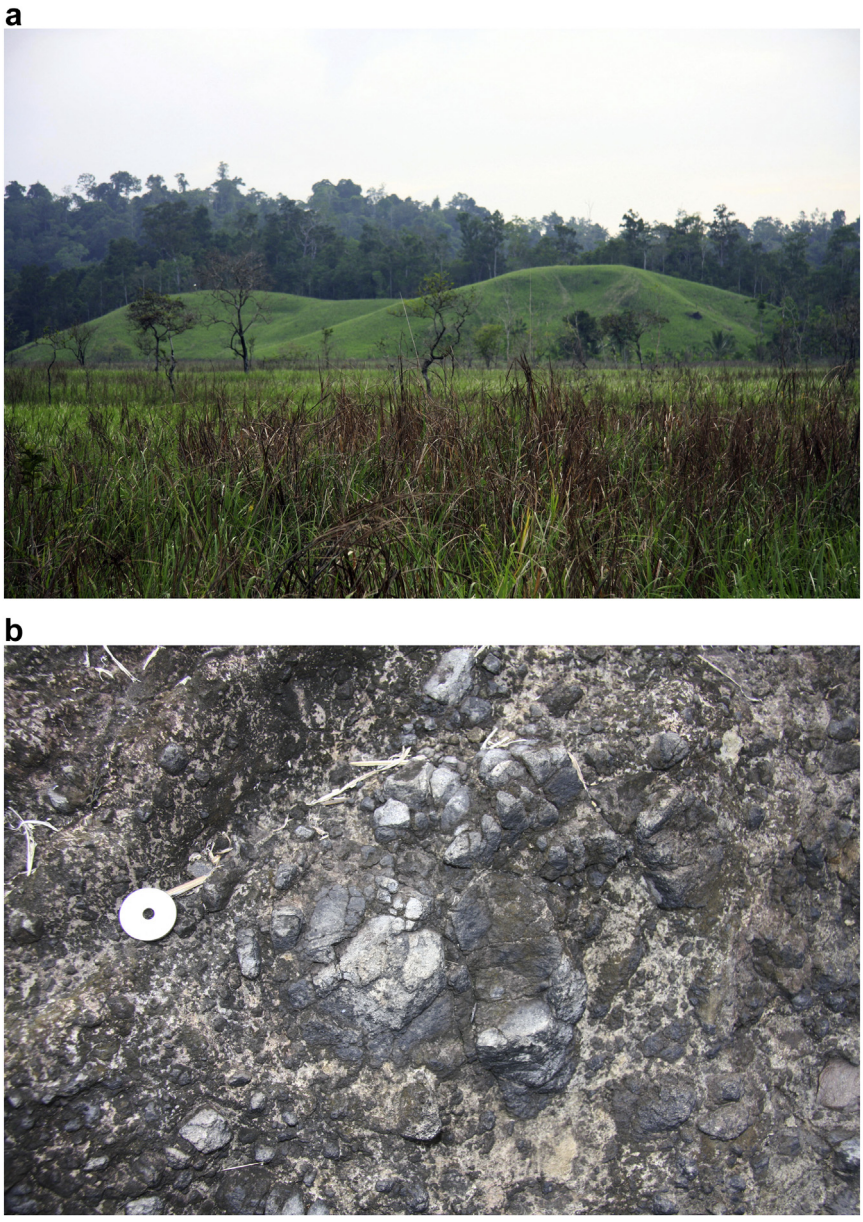

Fig. 4. Deposit of 20,000 BP debris avalanche associated with formation of the pre-1951 horseshoe-shaped crater of Mount Lamington: (a) hummocks up to 15 m high on the surface of the DA deposit. Embi Lakes are behind the hummocks. (b) Fractured rock fragments with "jigsaw puzzle" texture (terminology after Glicken, 1986) in the DA deposit. Coin (diameter 3.3.cm) for scale. Photos by A. Belousov.

On January 17 the earth tremors became almost continuous, and the first ash emission was noticed in the steam column. We interpret this and the following ash emissions as the vulcanian type explosive activity (in a broad sense after Clarke et al., 2015). It was probably caused by explosive interaction of the rising batch of magma with groundwater, or/and by explosive exsolution of gases from the magma batch.

On January 18 it was first noticed that the ash column originated from the top of a new dome-like structure. Taylor (1958) cited Mrs. Cowley: "By midday a large hill built itself up between the hills at the foot of Mount Lamington and the mountains in the rear. It was from the top of this hill that the ash was now issuing in terrific force, and flowing over the sides was steamy white cloud which we couldn't distinguish even with a telescope, but it didn't come more than about one third of the way down the newly built hill." Taylor interpreted the hill as a cone of the ejected fragmental material surrounding the volcanic vent. However, the eyewitness' description fits more to a dome: either a new small lava dome or slope bulge associated with cryptodome intrusion. The additional argument supporting such interpretation is that the explosive activity observed at the time (Fig. 5) (phreatomagmatic vulcanian outbursts) is characterized by wide

Fig. 3. Edifice of Mount Lamington: (a) before and (b) and (c) after the 1951 eruption. (a) in 1947, looking eastward. From Taylor (1958). (b) in January 30, 1951, looking southward. From Taylor (1958). (c) in August 1982, looking southward. Photo by R.Hoblitt.

Table 2
Observations of activity before and during the January 21, 1951 eruption of Mount Lamington (summarized from Taylor, 1958 and 1983).

Date	Location and Eyewithness	Observed event	Interpretation
Beginning of 1951	Sangara Plantation	Occasional small tremors.	New batch of magma starts to rise upward under the volcano.
January 15, Monday	Sangara Plantation	Landslides as brown streakes in the forest of the steep slopes.	The rising magma batch reaches shallow level and disturbs ground water table, increases pore pressure in rocks of the volcanic edifice.
	Sangara Plantation (Mrs. Henderson)	Thin column of smoke rising from the base of the Lamington Peaks.	Boiling of groundwater and degassing of the magma batch.
January 16, Tuesday	Waseta, Sangara, Higaturu (Mrs. Cowley)	30 shocks in 12 h when the whole earth rocking.	Strong deformations of the volcanic edifice accompanying formation of cryptodome.
	Sangara Plantation (Mr. Gwylt)	More extensive landslides moved down the slopes of the inner peaks and removed much of vegetation.	
	Higaturu	Vapor column was seen above volcano.	
January 17, Wednesday	Higaturu (Mr. James)	Earthquakes occurred with monotonous regularity (a shock every 7-min).	
	Sangara (Miss de Birba)	A steady stream of vapor with light ash above the crater.	Beginning of vulcanian type explosions.
January 18, Thursday	Higaturu, Issivita, Waseta, Awala.	"Almost incessant" strong earthquakes, people could not sleep.	
	Higaturu (Mrs.Cowley)	By midday a large hill built itself up between the hills at the foot of Mount Lamington and the mountains in the rear. It was from the top of this hill that the ash was now issuing in terrific force.	Bulging of slope above the cryptodome or formation of small lava dome.
	Sangara (Miss de Birba), Higaturu (Ivan Champion)	The great thick puffs of smoke curling in cauliflower shape was gushing forth to a great height (Fig. 5).	Explosive interaction of the magma batch with ground water (phreatomagmatic explosions).
	Issivita (Father Porter), Sangara Plantation (Mr. Henderson, Mr.Gwilt).	Flashes of light were visible intermittently in this vast column, with noises which sounded like thunder. The whole sky was alive with electric activity.	Lightnings in the ash clouds of the phreatomagmatic explosions.
	Higaturu (Mr.James)	Rumbling could be heard both before the eruption and afterwards. There was a flow of something in one of ravines.	Mudflow connected with expelling of ground water from the volcanic edifice.
	Issivita (Miss Reay)	Some buildings collapsed because of strong earthquakes.	
January 19, Friday	Waseta (Miss Reay)	In the morning great column of smoke in the direction of Waseta, stones were fallen.	
	Yodda (Mr.Kienzle)	Black cloud issuing out with a fast rate but not reaching higher than 5 km.	
	Sangara (Mr. Gwilt)	Definite subterranian grumblings heard, after rumble the smoke belched from crater. This procedure continued all day and night.	
	Waseta (Miss Reay).	Stench of volcano was unbearable.	Degassing of the magma batch emplaced at shallow level.
	Kokoda (Mr. Yeoman)	Luminous effects in the column at night.	
	Sangara (Miss de Birba)	New vents (four or five) opened in the crater.	
	Yodda (Mr. Kienzle), Issivita (Father Porter)	Continuous stream of smoke up to height of 8 km. The smoke was much denser as before.	
January 20, Saturday	Jegerata (Mr.R.Hart)	Rumbling composed of rapid succession of separate explosions blended into continuous pattern of sound.	
	Yodda (Mr. Kienzle), Sangara Plantation (Mr. Henderson)	At night "fireballs" or "whirling stars" in the column. Earthquakes almost stopped at 20:00.	Outbursts of incandescent material.
January 21, Sunday		In the morning no great change in the activity.	
Before 10:40 AM	Sangara (Mrs. Stephens)	Before the climatic explosion the area low on the NE slopes bursting forth into cloud and smoke.	Possible PF (?)
10:40 AM	Issivita	During first 3 min the long continious roar which with time increased in volume.	Climactic explosion
	Pilot of QANTAS Captain Jacobson.	Black mushroom-shaped explosion on the height >15 km and black cloud whirling and billowing like an oil fire in NW, N and NE directions.	

dispersion of the erupted material (Walker, 1973) and commonly forms around the vents rather low profile tuff rings (not cones). So at Lamington small dome was probably observed.

On January 18 the ash column was several km high (Fig. 5), varied in spasms from grey to black color, obtained a cauliflower shape and was accompanied by frequent lightning. During next days several more vents appeared. Taylor cited Miss Margaret de Birba: "The first day there seemed to be only one crater, but on the next there were more, and on the third day, four or five, apparently in the area of the original crater, inside the circle of peaks". The earthquakes became so strong and frequent that people could not sleep in Higaturu. A mudflow was seen in one of the ravines on the volcano slope.

On January 19 further increase of the explosive activity occurred; stones (probably lithic lapilli) were reported falling in Issivita area, and earthquakes were so strong that some buildings collapsed.

On January 20 black cauliflower column rose up to the height of 8 km, and new vents opened in the crater. Early in the morning on January 21 activity of the volcano continued on the same high level, however no earthquakes were felt. A new phenomenon, possibly indicating formation of small PFs, was observed: "a small area to the

Fig. 5. Preclimactic activity on January 18, 1951: ash-laden cloud of vulcanian explosion about 1 km high. Signed on the opposite side of the photo: "I took this snap a few minutes after the first blow, Allan Champion". Courtesy Fryer Library, University of Queensland, Australia.

left (of the crater) and much lower on the slopes burst forth into cloud and smoke" (Taylor cited Mrs. Stephens).

4.2. The January 21 climactic explosion and PDC

Transition from the pre-climactic vulcanian activity to the climactic explosion occurred suddenly at 10:40 am on January 21 (Taylor, 1958; Johnson, 2013, 2020). The long continuous roar which with time increased in volume was heard during the first 3–4 min in Issivita and black cloud whirling was seen in Sangara. The explosion was observed and photographed from the ground as well as from two flying-by QANTAS aircrafts that were in nearby airspace (Fig. 6). Most informative are observations and a sequence of four photographs taken by Captain Jacobson from a Douglas DC 3 aircraft flying at altitude of 3 km. These photos clearly show that the explosion was initially directed straight upward (Fig. 6a), but within several seconds part of the ash cloud lost buoyancy and started to collapse downward. When it reached the ground it spread radially in the form of a blast PDC (Fig. 6b). In 20 min, the black mushroom-shaped column rose to a height of 15 km and its base rapidly expanded as if "the whole countryside were erupting". Mr.Urquhart from the second Qantas flight caught the first moments of the cloud radial spreading (Fig. 6c).

The velocity of the cloud moving along the ground surface was so high that only people near the edges of devastated areas were able to escape. Ross Biddulph (the pilot of the second Qantas plane - De Haviland DH84 'Dragon') estimated the propagation velocity of the blast PDC as twice that of the aircraft 2×67 km/h $= 135$ km/h $= 37$ m/s (Qantas,

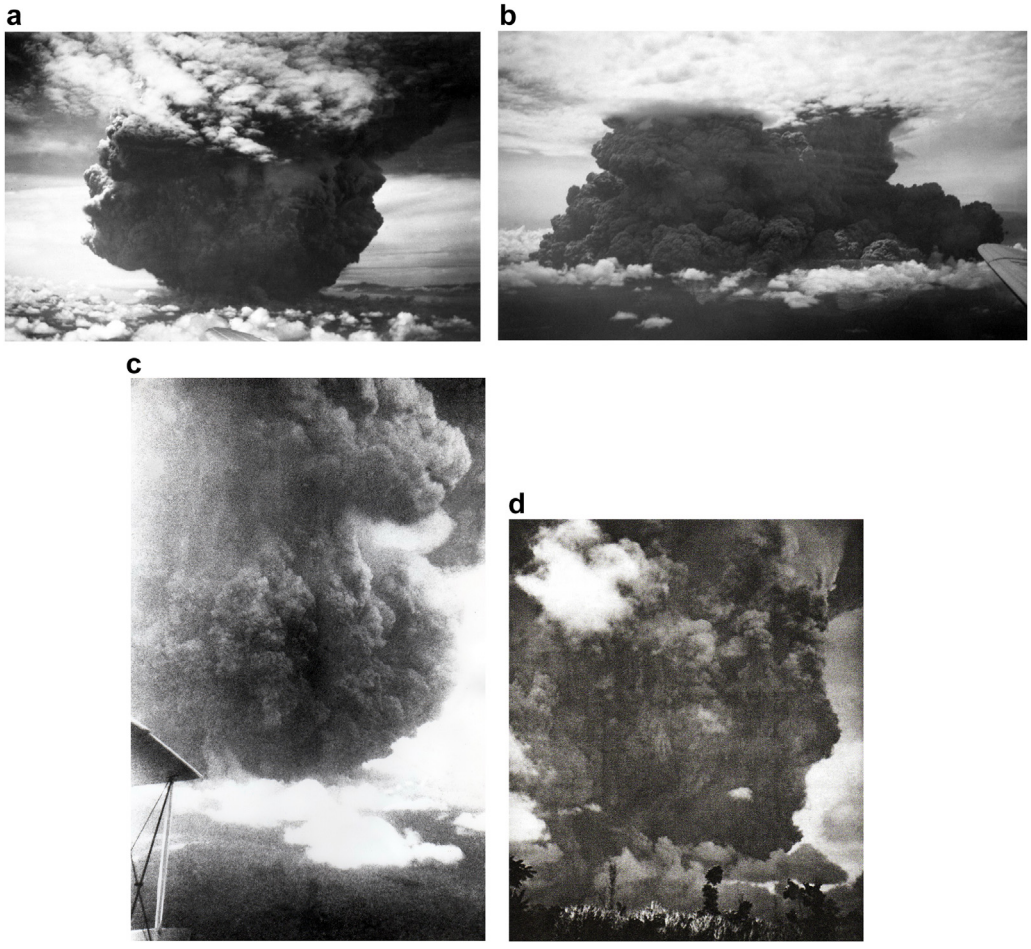

Fig. 6. Climactic explosion on January 21, 1951. Photos (a) and (b) by Captain Jacobson, from DC3 aircraft: (a) initial vertical cloud; (b) several seconds later: radial spreading of the eruption cloud with formation of the blast PDC ("ash hurricane"). Photos courtesy National Library of Australia. (c) initiation of radial spreading of the PDC cloud. Photo by Mr.Urquhart from Qantas, De Haviland DH84 'Dragon' aircraft (probably taken sometime in-between the moments when photos (a) and (b) were taken). (d) The only existing photo of the climactic explosion taken from the ground (from Popondetta airfield area). First published in "Illustrated London News" on February 24, 1951. Photo by Mr. Fred Senior Kleckham.

1951). Taylor (1958) provides two other independent estimations of the velocity: 27–94 m/s (based on the time reported by local residents that it took for the PDC to reach their settlements) and 70–80 m/s based on calculation of wind velocity needed to produce the tree blow-down and other observed destructions (Fig. 7).

Later the same day (January 21) at about 8:30 PM, a second violent eruption occurred at the volcano. This eruption was loud, producing a great deal of volcanic fallout, and the ash cloud may have risen as high as the one in the morning (Johnson, 2013). This explosion was not accompanied by notable PDCs and is not considered in the paper.

4.3. Post-climactic activity

Post-climactic activity of Mount Lamington included extrusion of a lava dome inside the new horseshoe-shaped crater. This was accompanied by several explosive episodes that produced pyroclastic flows, the most significant of which occurred on March 5, 1951. By the end of the post-climactic eruptive period the new lava dome partially filled the 1951 crater. The period of repeated lava dome building and collapse with emplacement of pyroclastic flows and lahars continued from 1951 to 1953. The dome reached a height of 450 m above the crater floor and a volume of approximately 0.2 km^3 (Fig. 3c; Haantjens et al., 1964).

5. Reinvestigation of the 1951 deposits

5.1. Deposits of the 1951 blast PDC

As noted by Taylor (pp.63–64 from Taylor, 1983), the deposit of January 21, 1951 climactic eruption consisted of a relatively thin, extensive component that covered the entire devastated area (the deposit of "ash hurricane") (Fig. 8) and relatively thick "ponderous ash flow nuee ardentes" that filled some river valleys (Fig. 9).

In the course of our field work at Mount Lamington conducted in 1982 (Hoblitt, 1982) and then in 2010 we found that in distal areas, where the blast PDC deposit (the deposit of "ash hurricane") is only a few cm thick, it is extensively bioturbated and discontinuous. However, in more proximal areas where the deposit is thicker, we found numerous locations (Fig. 1b), where it was not strongly reworked/bioturbated during the >30 years that had passed since the eruption. The blast PDC deposit still retained most of the original depositional features, e.g. internal layering and grain size variations. The deposit was commonly found in shallow pits we dug on interfluves covered by dense tropical forest, which has completely recovered since the eruption. The deposit consists of tens of centimeters of normally graded grey ash and lapilli (Fig. 8a). The layer is underlain by pre-1951 organic-rich brown soil and is overlain by poorly-developed modern soil and forest duff up to 10 cm thick that accumulated after the deposit was emplaced.

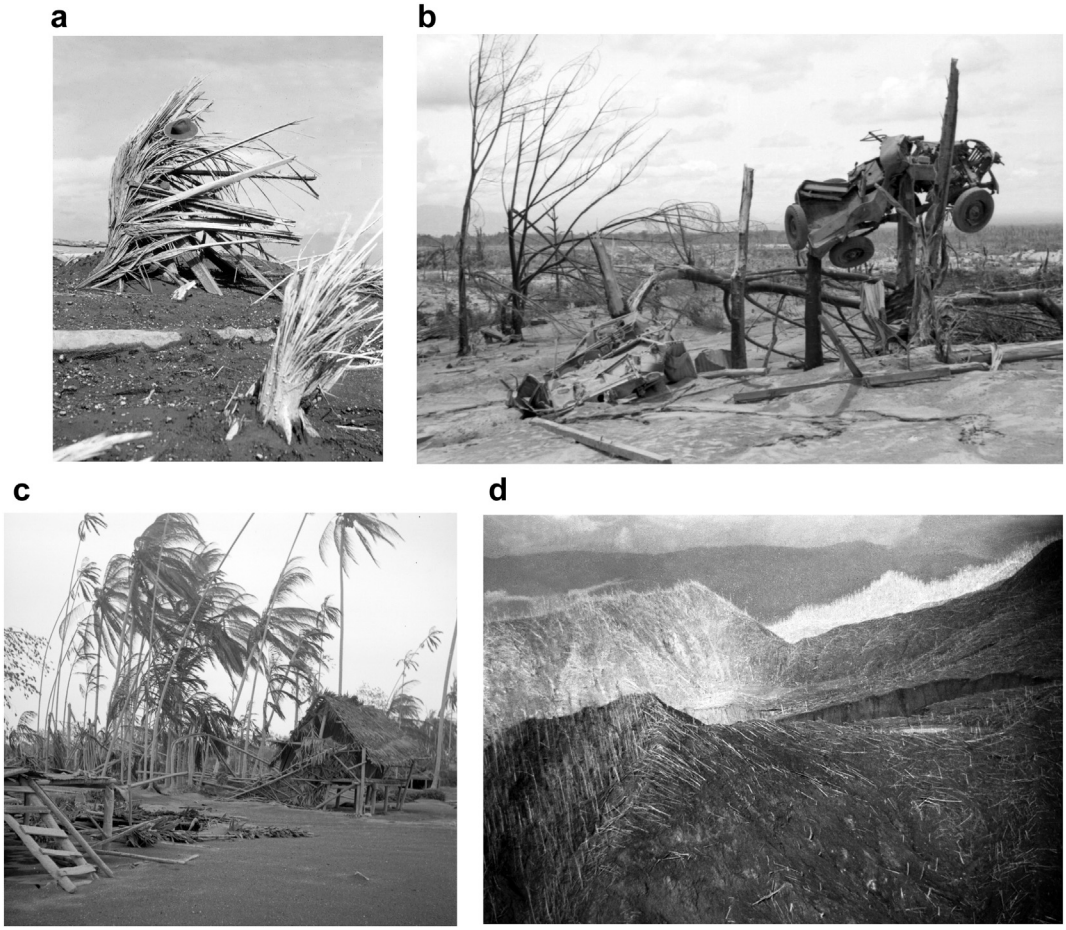

Fig. 7. Effects and deposit of the 1951 blast PDC ("ash hurricane"). Photos from Taylor (1958). (a) in the proximal area: smashed and abraded stumps of the trees knocked down and carried away by the "ash hurricane". (b) jeep thrown on the top of truncated trees, Higaturu, 9 km from the volcano. (c) the palm trees were singed but left standing in the distal area. Note thin veneer of the fine-grained "ash hurricane"deposit on the ground. (d) pattern of the blow-down forest; trees remained standing in areas protected by topographic obstacles.

As Taylor suggested (pp.64–65 from Taylor, 1983), the deposit can be naturally subdivided into two major stratigraphic units. However, subdivision into three units is more appropriate in proximal areas (Figs. 8a and 10). The contacts between units are gradational. A coarse, friable lower zone (about 10 cm) that is brown in color and appears to incorporate pre-existing soil; a middle zone (about 10 cm) that is coarse, friable and dark grey in color (due to the dearth of fine particles); and an upper zone that contains enough fine ash to be somewhat cohesive and lighter in color.

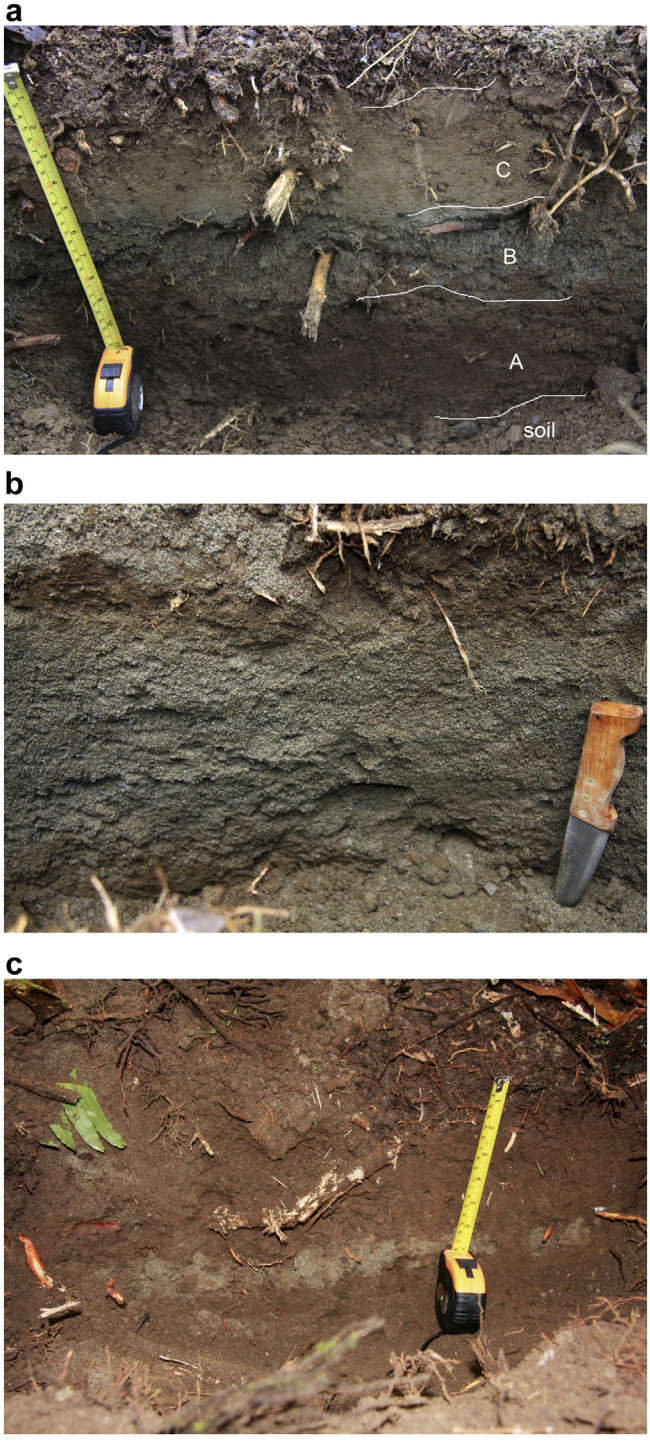

Fig. 8. Photos of the 1951 blast PDC ("ash hurricane") deposit, by A. Belousov. (a) Proximal area, point #11 at distance 6 km from the volcano. The deposit consists of 3 layers: layer C (the uppermost) - light colored, and fine grained; layer B (middle) - grey, fines depleted, coarse ash and fine lapilli; layer A (the lowermost) - brownish part of layer B mixed with picked up soil. (b) Medial area, point #1 at distance 9 km from the volcano: one layer of grey coarse ash with thickness about 15 cm. (c) Distal area, point # 17 > 10 km from the volcano: one 2 cm-thick layer of grey fine ash. Locations of the points see in Fig. 1b.

Fig. 9. The 1951 secondary pyroclastic flow deposit ("ponderous ash flow nuee ardente" of Taylor), Herman Patia as a scale. Ambogo River, distance from the crater is about 7 km. Photo by A.Belousov.

Based on stratigraphic characteristics and grain size (Figs. 10 and 11) we attribute the lower, middle, and the upper zones correspondingly to the layers A, B and C that are characteristic for deposits of the classic blast PDCs (Belousov, 1996). One apparent difference, however, is the absence of organic debris in the basal unit of the deposit of Lamington's blast PDC, because organic debris is abundant in the basal unit of the Mount St. Helens blast PDC deposit. A likely explanation is that such material was present in the fresh deposit but have since rotted away. Evidence supporting this explanation was found in some low mounds at the point PNG 9 (Fig. 1b). When we dug into the mounds, we found that they contained numerous elongate voids. Apparently the mounds were heaps of shattered wood and ash; the wood has since been removed by various organisms. Further evidence of this explanation is that wood debris is now rapidly rotting away in the basal unit of the Mount St. Helens' blast PDC deposits.

Taylor (Fig. 81 from Taylor, 1983) in the base of the blast PDC deposit (of his "ash hurricane" deposit) in proximal areas described a peculiar layer 15 cm thick composed of red ash containing plant fragments and water-worn stones. He attributed this basal layer to the deposit of the

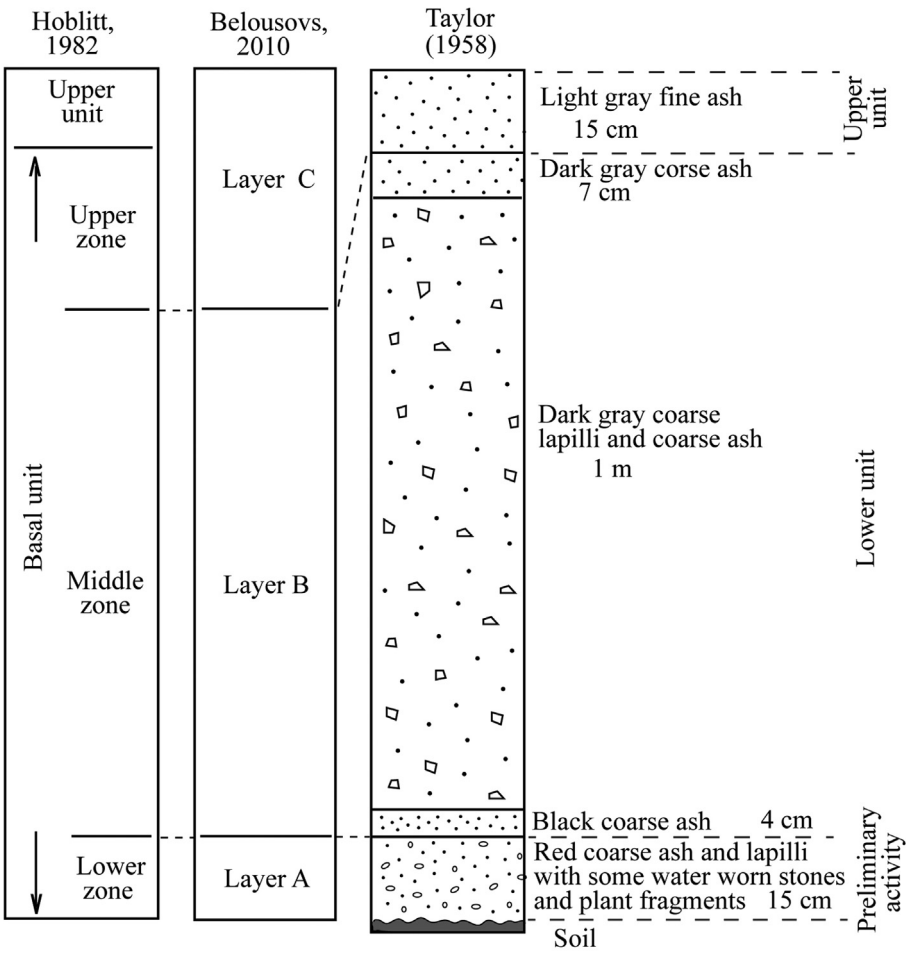

Fig. 10. The best-fit correlation of stratigraphy of the 1951 blast PDC ("ash hurricane") of Mount Lamington suggested by Taylor (1958), Hoblitt (1982) and Belousovs in 2010.

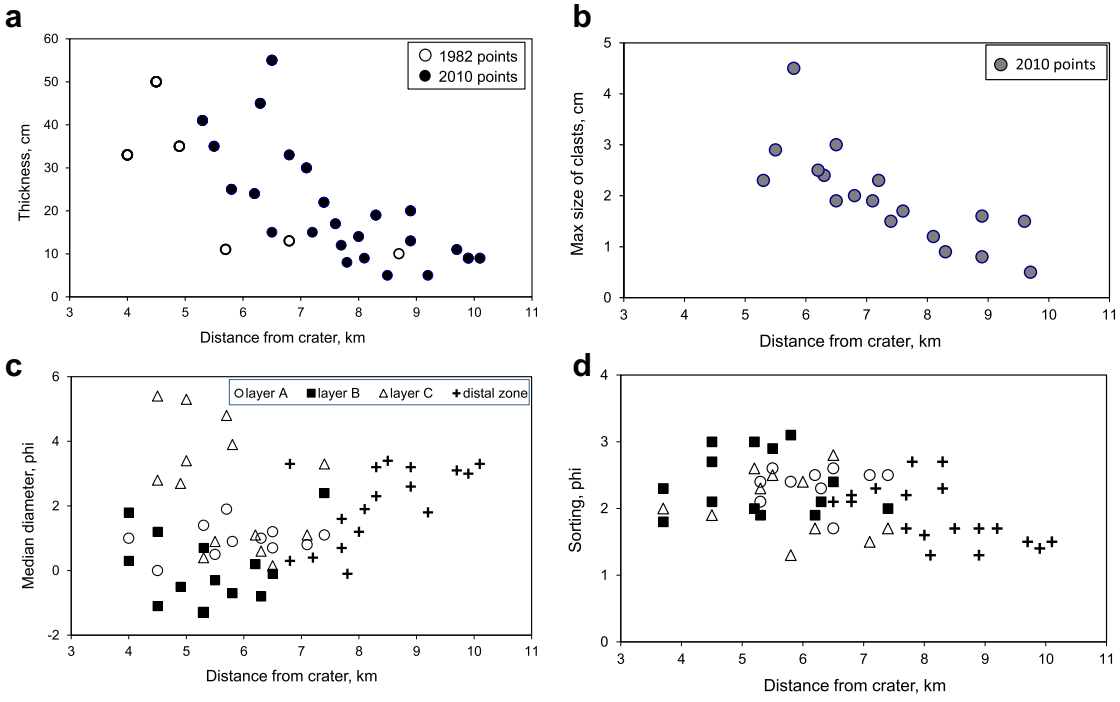

Fig. 11. Characteristics of the 1951 blast PDC ("ash hurricane") deposits versus distance. (a) Thickness. (b) Maximum diameter of juvenile fragments (average of ten largest rock fragments). (c) Median diameter after Inman (1952). (d) Sorting after Inman (1952). For (c) and (d) figure captions are the same.

Table 3
Average grain size characteristics of the 1951 blast PDC ("ash hurricane") deposit of Mount Lamington.

	Proximal zone			Distal zone
	Layer A	Layer B	Layer C	
Distance from crater, km	10-Apr	4–9.5	4.5–10	7–10.5
Amount of samples	20	12	19	9
Md (phi)	1.1	0.6	3	1.5
Sorting (phi)	2.2	2.1	1.9	2
Lapilli (>2 cm), %	19	31.7	10.6	15.8
Coarse ash (0.1 mm-2 cm), %	73.5	65.5	58	75.1
Fine ash (<0.1 mm), %	7.5	2.8	31.4	9.1

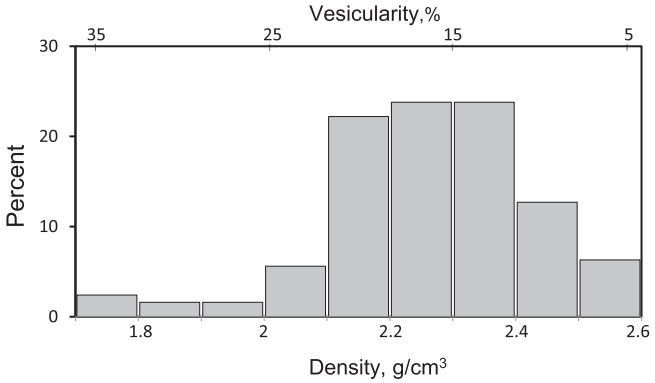

Fig. 12. Density/vesicularity distribution of juvenile andesite fragments of the 1951 blast PDC deposit of Mount Lamington.

preclimactic activity. However, the admixture of plant fragments and other material of the substrate indicates that this layer could be attributed to the layer A of the blast PDC deposit.

The uppermost unit is the most fine-grained unit in any section; in some sections this unit seems to contain traces of accretionary lapilli. Taylor reported the presence of pisolites in the upper part of the "ash hurricane" deposit so we assume that they were much more apparent in the fresh deposit. This is also true of the Mount St. Helens blast PDC deposit: pisolites were much more apparent in the newly-emplaced deposit than they are today. This unit corresponds to the accretionary lapilli unit of Mount St. Helens (Hoblitt et al., 1981); and to the uppermost part of the layer C of Bezymianny blast PDC deposit (Belousov, 1996).

Stratigraphic characteristics of the 1951 blast PDC deposit exhibit strong local variations, but its thickness and grain-size have clear trends with distance from the volcano (Fig. 8b and c). At distances from 3 to 10.5 km, the maximum deposit thickness decreases from 55 to 5 cm (Fig. 11a), the average size of the 10 largest juvenile clasts decreases from 4.5 cm to 0.5 cm (Fig. 11b), the Md diameter decreases from −1.3 to 4.8 phi (Fig. 11c), sorting improves from 3 to 1.3 phi (Fig. 11d, Table 3).

The most distal outcrops of the blast PDC deposit that we found were at distances of 10–11 km from the volcano. The deposit was probably too thin to be preserved at more distant locations. At point #1 (Fig. 8b), 9 km from the volcano and 2 km from the outer boundary of the devastated area, the deposit of blast PDC forms a discontinuous structureless layer of up to 15 cm thick in brown soil at depth of 10 cm.

The blast PDC deposit consists of 80% juvenile andesite fragments (Table 4), representing the explosively fragmented dome/cryptodome, and 20% accidental rock fragments of the old volcanic edifice. The juvenile andesite is highly crystalline and poorly vesiculated with a unimodal density distribution ranging from 1.7 to 2.6 g/cm^3 with a peak value between 2.1 and 2.4 g/cm^3(Figs. 12 and 13).

The area covered by the 1951 blast PDC deposit is 230 km^2 (Taylor, 1958). Assuming an average deposit thickness of 10–15 cm, its volume is about 0.025 km^3. Using the percentage of juvenile clasts in the deposit (80%), the average bulk density of the deposit as 1.5 g/cm^3 and the density for the andesite magma as 2.7 g/cm^3, we calculate that the volume of the cryptodome/ lava dome that experienced explosive fragmentation on January 21, 1951 was about 0.01 km^3.

5.2. The 1951 debris avalanche deposit

Analysis of the set of aerial photographs taken by the Royal Australian Air Force on February 5, 1951 revealed what appeared to be a hummocky flowage deposit (Fig. 14a) north-northeast of the crater. This deposit is also visible on several terrestrial photos, taken soon after the eruption (Fig. 14b). The deposit morphology closely resembles the morphology of fresh debris avalanche.

The deposit terminus is about 1–1.5 km west-northwest of Banguho village (Fig. 1b). In 2010 we managed to cross the area of interest but unfortunately it was densely vegetated and we found no good outcrops. However, we identified the characteristic hummocky terrain with scattered meter-sized angular fragments of lavas of the old volcanic edifice of Mount Lamington (Fig. 14c). This allowed us to confirm that the suspected debris avalanche deposit in Fig. 14a is indeed the product of the 1951 sector collapse.

The approximate length of the 1951 debris avalanche deposit is 8.5 km, its width is 1.5 km, and its area is 13 km^2. Using the average thickness of 2–3 m, the debris avalanche volume is 0.02–0.04 km^3.

6. Discussion

Preclimactic activity before the January 21, 1951 explosion of Mount Lamington in many aspects resembles the preclimactic activity observed before blasts of Bezymianny in 1956, and Mount St. Helens in 1980 (Table 5). In the Bezymianny and Mount St. Helens examples, the preclimactic activity was associated with the slow ascent/ intrusion

Table 4
Major and trace elements concentrations in juvenile andesite of the 1951 eruption of Mount Lamington. Samples: blast – deposit of the blast PDC, dome – post 1951 dome. XRF analyses made by Axios Advanced XRF spectrometer with 4 kW·Rh tube in Earth Observatory of Singapore.

	SiO_2	TiO_2	Al_2O_3	Fe_2O_3	MnO	MgO	CaO	Na_2O	K_2O	P_2O_5	Loss	SUM-(S)	S
Blast	59.88	0.62	17.3	5.24	0.104	3.18	5.69	4.35	2.15	0.239	0.55	99.27	<0.01
Dome	59.76	0.67	16.7	5.64	0.111	3.67	5.78	4.31	2.21	0.255	0.2	99.29	<0.01

	Sc	Ba	V	Cr	Ni	Cu	Zn	As	Rb	Sr	Y	Zr	Nb	Mo	Sn	Pb	Bi	U	Th	La	Ce	Nd
Blast	12.9	732	108	65.3	24.3	15.3	61.2	3.5	51.3	942	16.5	149	3.5	0.7	<1	##	<2	<2	5	23.1	44.1	16.3
Dome	14.4	725	122	107	29.4	25.3	65.7	<3	53	858	17.5	158	3.8	1	<1	##	<2	<2	5.7	21.4	42.6	18.9

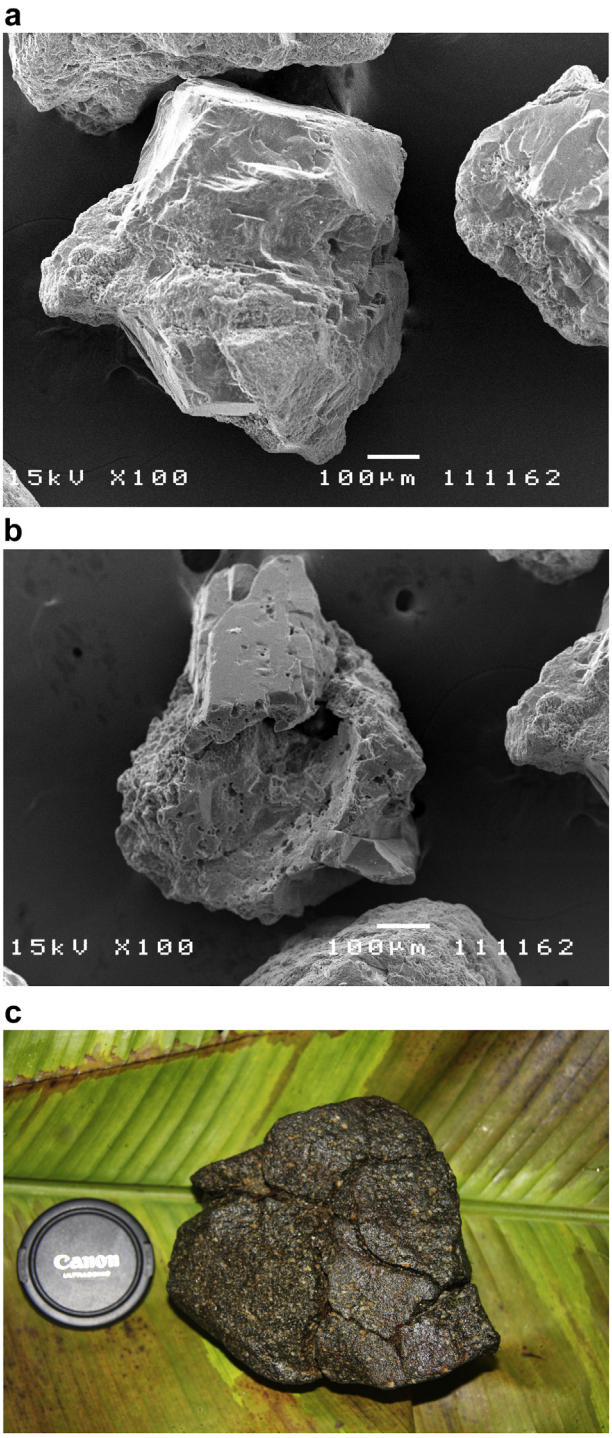

Fig. 13. Juvenile andesite of the 1951 blast PDC of Mount Lamington. (a and b) SEM images of sand size particles. (c) bomb with poorly developed bread crust surface.

of highly viscous magma into shallow levels beneath as well as inside the edifices of the volcanoes. Thus it is plausible to conclude that at Mount Lamington the climactic explosion was also preceded by shallow intrusion of magma. At Mount Lamington, it is unclear from visual observations alone whether the intruding magma body reached the ground surface before the January 21 paroxysm. The "new hill" described by observers on January 18 (Table 2) could have been a small subaerial lava dome, a bulge of old edifice material pushed up by a growing subsurface cryptodome (as at Mount St. Helens), a mound of ejecta, or some combination of these. The description of the phenomenon resembling a pyroclastic flow early in the morning on January 21 indicates that magma probably reached the ground surface shortly before the climactic explosion. This conclusion is supported by the density/ vesicularity distribution of the juvenile andesite fragments in the Lamington blast deposit. Their low overall vesicularity and unimodal distribution indicate that prior to explosive fragmentation the rising magma had experienced significant cooling, degassing and crystallization. Consequently, during catastrophic explosive fragmentation the additional vesiculation is minimal (Neill et al., 2010). Bread crust surfaces are rare and poorly developed in the juvenile fragments of the Lamington blast deposit (Fig. 13b), supporting interpretation of shallow pre-eruptive storage.

A similar range of vesicularity in combination with its unimodal distribution was found in juvenile material of the Boxing Day blast of Soufriere Hills, Montserrat in 1997, which was produced by explosive fragmentation of a superficial lava dome (Belousov et al., 2007). In contrast to the Soufriere Hills and Mount Lamington cases, juvenile materials of blasts of Bezymianny and Mount St. Helens, which originated mostly from fragmentation of subsurface cryptodomes, demonstrate much wider ranges of vesicularity, bimodal distributions, as well as common breadcrust surfaces (Belousov et al., 2007). However, the lower vesicularity of the blast material of Lamington could be explained by relatively small volume of the cryptodome of Mount Lamington (Table 5), and the consequent high surface area to volume ratio. Thus, the existing data allow to conclude that at Mount Lamington during the pre-climactic period the small shallow cryptodome was emplaced, part of which reached the ground surface in the form of small lava dome. Total volume of both was about 0.01 km^3.

In the case of Mount Lamington the pre-climactic activity lasted <1 week, while in the case of Bezymianny it lasted 23 weeks, and at Mount St. Helens it lasted 7.5 weeks (Table 5). The relatively short duration of the pre-climactic activity at Mount Lamington may have been caused by high gravitational instability of the volcanic edifice; i.e., the edifice collapse happened in the very beginning of the cryptodome intrusion. High instability of the pre-1951 Lamington edifice is likely because of its internal structure: it consisted of a lava dome built on the inclined floor of the 20,000 BP horseshoe-shaped crater. Such intracrater lava domes are typically unstable and exhibit frequent cycles of growth and collapse as described for many volcanoes worldwide, e.g. at Shiveluch, Harimkotan, Augustine volcanoes and Soufriere Hills, Montserrat (Voight et al., 1981, 2002; Begét and Kienle, 1992; Belousov, 1995; Belousov et al., 2007). Such internal structure of the pre-1951 edifice also predetermined the direction of the 1951 collapse that coincided with the direction of the previous collapse 20,000 BP.

In the Bezymianny and Mount St. Helens examples, the pre-climatic eruptive vents were located close to their respective summits. At Lamington, in contrast, pre-climactic deformation and venting apparently occurred near the base of the pre-1951 dome. This indicates that cryptodome growth at Lamington was relatively low in the edifice compared to the other examples (Fig. 16). An important question then is: could the 1951 avalanche deposit be the product of an eruption-triggering sector collapse event that unloaded the shallow magma body, i.e. was the Lamington paroxysm triggered in the same manner as the Mount St. Helens and the other classic blasts? This possibility would require that the hummocky debris found on Fig. 14a was mobilized shortly before, or when the blast explosion began. In this scenario, the debris would be deposited, depending on its velocity relative to the blast cloud, shortly before, during, or after passage of the blast-cloud front.

The time of emplacement of the terminus of the hummocky flowage deposit can be constrained by evidence on photographs. At the site of the DA flow terminus, the hummocky debris must have been emplaced after the passage of the blast cloud front because the terminus overlies trees that were toppled by that blast. We know that the debris was emplaced before February 5, when the photograph was taken. However,

Fig. 14. Photos of 1951 debris avalanche deposits of Mount Lamington. (a) Dark grey lobate front of the 1951 debris avalanche deposit (DA) overlaid by somewhat younger light grey pyroclastic flow deposit (PF), probably secondary blast PF. Aerial photography on February 5, 1951. (b) Albert Speer sitting in front of coarse-grained heterolithologic hummocky breccia (February 1951); probably the 1951 debris avalanche deposit in the area of point #DA1 in Fig. 1b. Steaming Mount Lamington and hills with blast-damaged forest in the background. (c) roots of post-1951 ceiba tree cover large angular boulder at the surface of the 1951 debris avalanche deposit, distance 6.5 km from the volcano, point #DA1 in Fig. 1b. Photo (a) and (b) courtesy National Library of Australia; (c) by A.Belousov.

the time of emplacement of the hummocky debris may be further constrained because a light-colored flowage deposit rests upon it (Fig. 14a). On the basis of morphology, the light-colored deposit could be the product of either a pyroclastic flow or a lahar. Of the two possibilities, a pyroclastic flow is more likely because a high moisture content tends to make fresh lahar deposits dark-colored. The light-colored deposit clearly was emplaced after the paroxysmal eruption. Emplacement could have occurred on the same day as the paroxysm, i.e., on January 21, or during a subsequent eruption that occurred before February 5. Taylor (1958) states that the first large post-paroxysmal eruption occurred on February 6. Thus, the light-colored deposit, if it is a pyroclastic flow deposit, probably was emplaced on January 21, the same day as the paroxysmal eruption. If so, the hummocky deposit on Fig. 14a was also probably emplaced on January 21. If the hummocky deposit is a product of a blast-triggering failure event, the photographic evidence indicates that the debris must have had a lower velocity than the blast cloud. This is analogous to the Mount St. Helens example, where the blast-triggering debris avalanche was overtaken by the blast cloud about 5 km from the vent. A similar sequence of events also took place during the 1956 eruption of Bezymianny volcano (Belousov, 1996; Belousov and Belousova, 1998).

The edifice collapse that triggered the blast on January 21 probably intersected the uppermost part of the intruding cryptodome. It exposed a subhorizontal surface of the cryptodome apex, while at Bezymianny, Mount St.Helens, and Soufriere Hills the rupture intersected the main body of the cryptodome/dome, and exposed their steeply inclined surfaces. Moreover, a significant part of the intersected magma bodies consequently became involved in the process of gravitational sliding, and thus produced strongly inclined and laterally extended explosions of the classic lateral blasts. The resultant explosion of Mount Lamington was thus directed vertically rather than laterally. Photographs of the Lamington explosion (Fig. 6) show that the eruptive cloud initially rose

Table 5
Comparative data for blasts of Mount Lamington, Bezymianny, Mount St. Helens and Soufrière Hills, Montserrat (after Belousov et al., 2007). * according to Taylor (1958), ** according to Clynne et al. (2008).

	Mount Lamington, 1951	Bezymianny, 1956	Mount St.Helens, 1980	Soufriere Hills, Montserrat, 1997
Characteristics of volcanic edifices				
Age of volcanoes, years	100,000	11,000	300,000**	>30,000
Ancient failures: amount/age	1/20,000	0	3**	1/4000
Ancient blasts: amount/age	0	0	1/990**	0
Repose before blast, years	2500	1000	123	400
Composition	andesite	andesite	dacite	andesite
Relative altitude, m	450*	1300	1700	1000
Height before/after, m	1800/1680	3085/2886	2951/2549	1030/650
Vent height reduction	400	750	900	300
Crater after eruption, km	1.3	1.7 × 2.8	2.8 × 3.5	0.4 × 0.5
Pre-climactic stage of eruption				
Dome/cryptodome V, km^3	0.01	0.15–0.2	0.11	0.035
Deformations, days-months	5 days	2–6 months	2 months	1.5 months
meters		100	150	
Volcanic activity	Phreatic - phreatomagm.	Phreatomagm- magmatic	Phreatic - phreatomagm.	Magmatic
Climactic stage of eruption				
Debris avalanche				
Drop height H, km	1.2	2.4	2,25	1
Travel distance L, km	8.5	22	25	4,5
Coefficient H/L	0.14	0.12	0,1	0.22
Area, km^2	13	36	64	1.7
Volume (V), km^3	0.02–0.04	0.5	2.5	0.05
Landslide V/edifice V	0.1	0.1	0.1	0.2
Velocity, m/s	<37	<60	50–70	>27
Directed blast				
Opening angle of devastation zones (degree)	360	110	180	70
Travel distance, km	13	30	27	>7
Area, km^2	230*	500	600	>10
Maximum thickness (m)	1*	2.5	2–2.5	3
Volume, km^3	0.025	0.2	0.11	0.03
Velocity, m/s	27–94*	>100	100–235	>100 initial
Boundary proximal/distal zone on axis (km)	7	19	15	>4
Temperature, °Celsium	200*	<250	100–350	~300
Average clast density (kg/m^3)	2260	2100	1660	2200
Average vesicularity (%)	16	20	30	15
Amount of juv.material, %	80	84	62	87
Post-blast eruption				
General characteristics	Semi-open-conduit	open-conduit	open-conduit	semi-open-conduit
Type of eruption	vulcanian explosions	pumiceous PFs	plinian eruption, PFs	vulcanian explosions
Post-climactic stage				
Growth of lava dome:	1951–1953	1956–until now	6 (1980–1986),	1997–until now
duration, years,	2	>63	5 (2004–2008)	17
volume, m^3	~0.2	>0.4	<0.1	>0.3

vertically but subsequently collapsed upon the terrain around the vent and spread laterally in a form of radially propagating PDC. The enhanced northward propagation of the PDC to a maximum distance of 13 km occurred due to redirection and focusing of the initially radially symmetrical PDC by the high walls of its 20,000 BP horseshoe-shaped crater, which was open to the north. Similar focusing of radial PDC propagation by a breached crater occurred in the course of the 1997 eruption of Bezymianny volcano (Belousov et al., 2002). Formally, the catastrophic vertical explosion of Lamington volcano could occur without the triggering edifice collapse, e.g. by mechanism suggested by Boudon et al. (2015), who proposed that similar explosion of Mt. Pelee in 1902 was associated with sealing of pore spaces of small dome of the volcano by cristobalite deposition and the dome overpressurization by volatiles ascending from the deeper part of the magmatic system. However, the finding of the debris avalanche of the 1951 eruption, provides more conventional and straightforward explanation for the triggering of the 1951 blast.

Stratigraphy of the 1951 PDC deposit is remarkably similar to that of the Mount St. Helens 1980 and the Bezymianny 1956 blast PDC deposits (Figs. 10 and 15). Layering similar to the typical A, B, C blast PDC stratigraphy is present in the proximal deposits of Lamington. However, the layers are not as clearly distinguished by grain size characteristics and lack the sharp contacts that are common in the deposits of the classic blasts (Belousov et al., 2007). We attribute this to the fact that, opposite to Mount St. Helens and Bezymianny examples, the Lamington blast cloud first ascended vertically before it collapsed and produced a PDC. Consequently, the PDC of Mount Lamington ingested more air and was more dilute than those at Mount St. Helens and Bezymianny. The difference may also be due to the fact that the Lamington explosion was smaller and less voluminous. "Ponderous ash flow nuee ardentes" that filled river valleys of the proximal area (Fig. 9) are similar in appearance to what was termed secondary pyroclastic flow deposits at Mount St. Helens (Hoblitt et al., 1981; Hoblitt and Miller, 1984) and Bezymianny (Belousov, 1996).

The reconstructed sequence of events of the 1951 eruption of Mount Lamington (cryptodome intrusion + edifice failure + blast with generation of the devastating blast PDC) are similar to those of "classic"

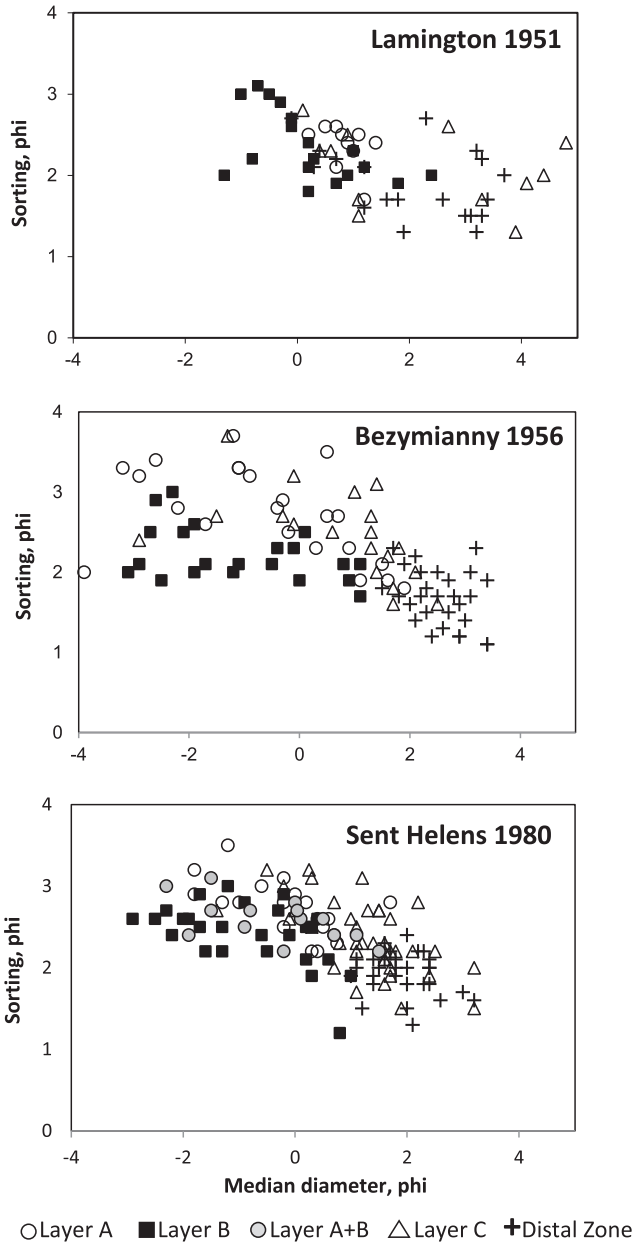

Fig. 15. Grain size characteristics of blast PDC deposits of Mount Lamington (1951), Bezymianny (1956) and Mount St. Helens (1980). (a) Percentage of lapilli (<−1 phi), coarse ash (from −1 to 4 phi) and fine ash (>4 phi). (b) Relationship between sorting and median diameter; coefficients after Inman (1952). Layer A + B the 1982 samples of R.Hoblitt with combined layers A and B.

directed blasts at Bezymianny, Mount St. Helens, and Soufriere Hills, Montserrat. Probably sector collapse of a volcanic edifice (even of a small scale) is a rather common (or possibly even the necessary) trigger of directed/lateral blasts. Hence we can conclude that deposits of blast PDCs are in characteristic association with deposits of debris avalanches. Thus temporal and spatial association of debris avalanches and directed/lateral blasts can help to distinguish deposits of blast PDCs in old volcanic successions (e.g. in cases when evidences of a PDC's high-velocity impact and emplacement have faded away). Moreover, we suggest to reserve the term "directed blast", as well as the term "lateral blast" specifically for volcanic explosions associated/triggered by volcanic landslides (and the term "blast PDC" for PDCs generated by such explosions).

The new and previously published data on eruptive history of Mount Lamington show that this volcano was very active during last 20,000 years, producing lava domes and PDCs of various types. Edifice of the volcano experienced two gravitational failures: major 20,000 BP and mild in 1951 CE. Internal structure of the present day edifice of Mount Lamington is nearly identical to the structure that this volcano had before the 1951 eruption. Thus it is plausible to suggest that in the case of renewal of activity of the volcano there is high probability of gravitational failure of its edifice similar to the one that occurred in the course of the last eruption. The character of explosive activity (lateral blast or vertical Plinian eruption) accompanying such gravitational failure will depend on the depth of the ascending magma body inside the volcanic edifice in the moment of failure and/or on relative position of the rupture surface of the landslide and the ascending magma body.

7. Conclusions

The reconstructed mechanism of the 1951 eruption of Mount Lamington (cryptodome intrusion + edifice failure + blast with generation of the devastating PDC) as well as the effects and characteristics of the blast PDC deposit are similar to those of "classic" directed blasts at Bezymianny, Mount St. Helens, and Soufriere Hills on Montserrat.

We attribute the salient differences (more symmetric area of devastation and less pronounced layering of the blast deposit) to the fact that the Lamington blast cloud first ascended vertically before it collapsed upon the terrain surrounding the vent and produced the blast PDC. Consequently, the blast PDC of Mount Lamington ingested more air and was more dilute than the "classic" blast PDCs. We suggest that the initial explosion was vertical because the rupture surface of the edifice collapse intersected the very tip of the intruding cryptodome.

We suspect that the relatively brief duration of the preclimactic activity at Lamington may have been caused by high gravitational instability of its central dome, which grew inside the 20,000 BP crater. The dome could withstand only weak disturbances (ground deformations, increase of pore pressure, seismic shaking etc.). Consequently, collapse occurred soon after magma intrusion began, while the cryptodome was still small and confined to a relatively deep level. Because of its small volume, the cryptodome was strongly degassed, densified and crystallized, so the vesicularity of the juvenile material in the resultant blast deposit was low.

Future eruption of Mount Lamington might repeat the scenario of the 1951 eruption. It will include gravitational failure of the 1951 intracrater dome followed by explosive eruption of the type that will depend on the depth of magma batch inside the volcanic edifice in the moment of failure as well as on relative position of the rupture surface of the landslide and the ascending magma batch.

Declaration of competing interest

The authors declare that they have no known competing financial interests or personal relationships that could have appeared to influence the work reported in this paper.

Acknowledgements

This research would not be possible without remarkable field assistance of volcanologist Herman Patia (Rabaul Volcano Observatory, PNG), who untimely passed away in 2012. Funding for field trip to Lamington in 2010 (for A.B., M.B. and H.P.) and analytic works was provided by Earth Observatory of Singapore (Nanyang Technological University) and for R.H in 1982 by USGS. Wally Johnson helped us to search data about the 1951 eruption in various archives in Australia. The National Library of Australia generously provided images taken by Taylor. Heather Wright, George Boudon and anonymous reviewer are

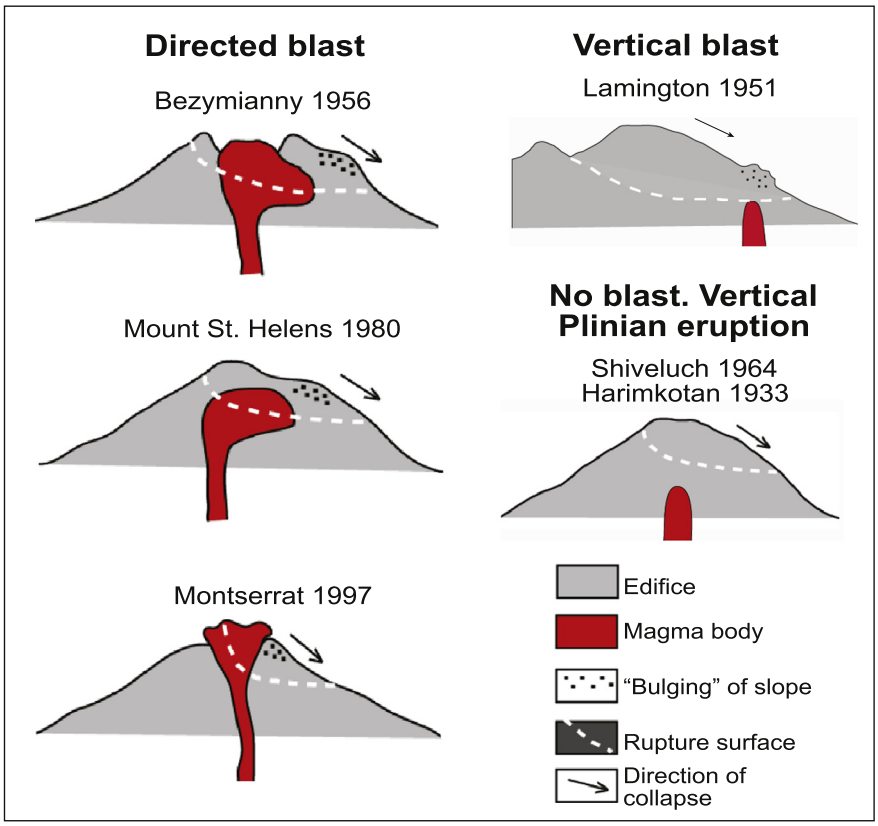

Fig. 16. Sketches illustrating positions of magma bodies inside volcanic edifices before gravitational collapses. In the case of directed blast: Bezymianny - combination of dome and cryptodome; Mount St. Helens - cryptodome; Soufrière Hills, Montserrat - dome, At Mount Lamington –rupture surface intersected the uppermost part of the cryptodome.

greatly acknowledged for the constructive reviews and comments, which helped to improve the quality of the manuscript. Any use of trade, firm, or product names is for descriptive purposes only and does not imply endorsement by the U.S. Government.

References

Arculus, R.J., Johnson, R.W., Chappell, B.W., McKee, C.O., Sakai, H., 1983. Ophiolite contaminated andesites, trachybasalts, and cognate inclusions of Mount Lamington, Papua New Guinea: anhydrite amphibole-bearing lavas and the 1951 cumulodome. J. Volcanol. Geotherm. Res. 18 (1–4), 215–247.

Baker, G., 1946. Preliminary note on volcanic eruptions in the Goropu Mountains, southeastern Papua, during the period December, 1943, to August, 1944. J. Geol. 54 (1), 19–31.

Baldwin, S.L., Fitzgerald, P.G., Webb, L.E., 2012. Tectonics of the New Guinea region. Annual Rev. Earth Planet. Sci. 40, 495–520.

Begét, J.E., Kienle, J., 1992. Cyclic formation of debris avalanches at Mount St. Augustine volcano. Nature 356, 701.

Belousov, A.B., 1995. The Shiveluch volcanic eruption of 12 November 1964 - explosive eruption provoked by failure of the edifice. J. Volcanol. Geotherm. Res. 66, 357–365.

Belousov, A., 1996. Pyroclastic deposits of March 30, 1956 directed blast at Bezymianny volcano. Bull. Volcanol. 57, 649–662.

Belousov, A., Belousova, M., 1998. Bezymyanny Eruption on March 30, 1956 (Kamchatka): Sequence of events and debris-avalanche deposits. Volcanol. and Seismol. 20, 29–47.

Belousov, A., Voight, B., Belousova, M., Petukhin, A., 2002. Pyroclastic surges and flows from the 8-10 May 1997 explosive eruption of Bezymianny volcano, Kamchatka, Russia. Bull. Volcanol. 64, 455–471.

Belousov, A., Voight, B., Belousova, M., 2007. Directed blasts and blast-currents: a comparison of the Bezymianny 1956, Mount St. Helens 1980, and Soufriere Hills, Montserrat 1997 eruptions and deposits. Bull. Volcanol. 69, 701–740.

Boudon, G., Balcone-Boissard, H., Villemant, B., Morgan, D.J., 2015. What factors control superficial lava dome explosivity? Sci. Rep. 5, 14551.

Clarke, A., Ongaro, T.E., Belousov, A., 2015. Vulcanian explosions. In: Sigurdsson, H., et al. (Eds.), The Encyclopedia of Volcanoes. Elsevier, pp. 505–518.

Clynne, M.A., Calvert, A.T., Wolfe, E.W., Evarts, R.C., Fleck, R.J., Lanphere, M.A., 2008. The Pleistocene eruptive history of Mount St. Helens, Washington, from 300,000 to 12,800 years before present.In a volcano rekindled: the renewed eruption of Mount St. Helens, 2004-2006. US Geological Survey No.

Cooper, P., Taylor, B., 1987. Seismotectonics of New Guinea: a model for arc reversal following arc-continent collision. Tectonics 6 (1), 53–67.

Fergusson, G.J., Rafter, T.A., 1953. New Zealand C^{14} age measurements. New Zealand J. Sci. Tech. 35, 127–218.

Glicken, H., 1986. Rockslide-Debris Avalanche of the May 18, Mount St. Helens, Washington. Ph.D. dissertation. University of California, Santa Barbara (303 pp.).

Gorshkov, G.S., 1959. Gigantic eruption of the Bezymianny volcano. Bull. Volcanologique 20, 77–109.

Gorshkov, G.S., 1963. Directed volcanic blasts. Bull. Volcanol. 26, 83–88.

Haantjens, H.A., Paterson, S.J., Taylor, B.W., Slatyer, R.O., Stewart, G.A., Green, P., 1964. General report on lands of the Buna-Kokoda Area, territory of Papua and New Guinea. Land Research Series No. 10, Commonwealth Scientific and Industrial Res. Org., Australia, Melbourne (115 p).

Hamilton, W.B., 1979. Tectonics of the Indonesian Region (No. 1078). US Govt. Print. Off.

Hoblitt, R.P., 1982. Reconnaissance of the Area Devastated by the January 21, 1951 Eruption of Mount Lamington, Papua: August 10–18, 1982 (Unpubl. admin. report, US Geol. Surv).

Hoblitt, R.P., Harmon, R.S., 1993. Bimodal density distribution of cryptodome dacite from the 1980 eruption of Mount St. Helens, Washington. Bull.Volcanol. 55 (6), 421–437.

Hoblitt, R.P., Miller, C.D., 1984. Comments and Reply on "Mount St. Helens 1980 and Mount Pelée 1902—Flow or surge?". Geology 12 (11), 692–693.

Hoblitt, R.P., Miller, C.D., Vallance, J.W., 1981. Origin and stratigraphy of the deposit produced by the May 18 directed blast. In: Lipman, P.W., Mullineaux, D.R. (Eds.), The 1980 Eruptions of Mount St. Helens, Washington. US Geol. Surv. Prof. Paper 1250, pp. 401–419.

Houghton, B.F., Wilson, C.J.N., 1989. A vesicularity index for pyroclastic deposits. Bull. Volcanol. 51 (6), 451–462.

Inman, D.L., 1952. Measures for describing the size distribution of sediments. J.Sediment. Res. 22 (3), 125–145.

Johnson W, R, 1987. Large-scale volcanic cone collapse: the 1888 slope failure of Ritter volcano, and other examples from Papua New Guinea. Bulletin of Volcanology 49, 669–679. https://doi.org/10.1007/BF01080358.

Johnson, R.W., 2013. Fire Mountains of the Islands: A History of Volcanic Eruptions and Disaster Management in Papua New Guinea and the Solomon Islands. ANU Press, Canberra.

Johnson, R.W., 2020. Roars from the Mountain: Colonial Management of the Volcanic Disaster at Mount Lamington in 1951. ANU Press, Canberra (in press).

Johnson, R.W., Mackenzie, D.E., Smith, I.E.M., 1978. Delayed partial melting of subduction-modified mantle in Papua New Guinea. Tectonophysics 46 (1–2), 197–216.

Lacroix, A., 1904. La Montagne Pelée et ses éruptions. Masson (662 pp).

Mueller, S., Scheu, B., Kueppers, U., Spieler, O., Richard, D., Dingwell, D., 2011. The porosity of pyroclasts as an indicator of volcanic explosivity. J. Volcanol. Geotherm. Res. 203 (3–4), 168–174.
Neill, O.K., Hammer, J.E., Izbekov, P.E., Belousova, M., Belousov, A., Clarke, A.B., Voight, B., 2010. Influence of preeruptive degassing and crystallization on the juvenile products of laterally directed explosions. J. Volcanol. Geotherm. Res. 198, 264–274.
Qantas, 1951. Operation Volcano. Qantas empire airways staff magazine, pp. 9–13 March-May.
Ruxton, B.P., 1966. Correlation and stratigraphy of dacitic ash-fall layers in northeastern Papua. J.Geol. Soc. Australia 13 (1), 41–67.
Siebert, L., 1984. Large volcanic debris avalanches: characteristics of source areas, deposits, and associated eruptions. J. Volcanol. Geotherm. Res. 22 (3–4), 163–197.
Smith, I.E., 1982. Volcanic evolution in eastern Papua. Tectonophysics 87 (1–4), 315–333.
Smith, I.E., 2014. High-magnesium andesites: the example of the Papuan Volcanic Arc. Geol. Soc, London, Special Publ. 385 (1), 117–135.
Smith, I.E.M., Compston, W., 1982. Strontium isotopes in Cenozoic volcanic rocks from southeastern Papua New Guinea. Lithos 15 (3), 199–206.
Smith, I.E.M., Johnson, R.W., 1981. Contrasting rhyolite suites in the late Cenozoic of Papua New Guinea. J. Geophys. Res. Solid Earth 86 (B11), 10257–10272.
Taylor, G.A.M., 1958. The 1951 eruption of Mount Lamington, Papua. Australia, Bureau of Mineral Resources, Geology and Geophysics 38 (117 pp).
Taylor, G.A.M., 1983. The 1951 Eruption of Mount Lamington, Papua. 2nd edition. 38. Bureau of Mineral Resources, Geology and Geophysics, Australia (129 pp).
Tregoning, P., Gorbatov, A., 2004. Evidence for active subduction at the New Guinea Trench. Geophys. Res. Lett. 31 (13).
Voight, B., Glicken, H., Janda, R.J., Douglass, P.M., 1981. Catastrophic rockslide avalanche of May 18. In: Lipman, P.W., Mullineaux, D.R. (Eds.), The 1980 Eruptions of Mount St. Helens, Washington. US Geol. Surv. Prof. Paper 1250, pp. 347–377.
Voight, B., Komorowski, J.C., Norton, G., Belousov, A., Belousova, M., Boudon, G., Francis, P., Franz, W., Sparks, S., Young, S., 2002. The 1997 Boxing Day sector collapse and debris avalanche, Soufrière Hills Volcano, Montserrat, B.W.I. In: Druitt, T., Kokelaar, B.P. (Eds.), The Eruption of Soufrière Hills Volcano, Montserrat, from 1995–1999. Mem. Geol.Soc. London. 21, pp. 363–407.
Walker, G.P., 1971. Grain-size characteristics of pyroclastic deposits. J.Geol. 79 (6), 696–714.
Walker, G.P., 1973. Explosive volcanic eruptions—a new classification scheme. Geol. Rundsch. 62 (2), 431–446.
Woodhead, J., Hergt, J., Sandiford, M., Johnson, W., 2010. The big crunch: physical and chemical expressions of arc/continent collision in the Western Bismarck arc. J. Volcanol. Geotherm. Res. 190 (1), 11–24.